6. Radiolabeled functional nanoparticles in preventive and regenerative medicine

Sanja Vranješ-Đurić[1], Nenad L. Ignjatović[2*]

[1] Laboratory for Radioisotopes, Vinča Institute of Nuclear Sciences, University of Belgrade, PO Box 522, 11001 Belgrade, Serbia

[2] Institute of Technical Sciences of the Serbian Academy of Science and Arts, Knez Mihailova 35/4, 11000 Belgrade, Serbia

* Corresponding author:

E-mail address: nenad.ignjatovic@itn.sanu.ac.rs; dr.nenad.ignjatovic@gmail.com (N.L. Ignjatović)

Abstract:

Radiolabeled nanoparticles (NPs) are finding an increasing interest in a broad range of biomedical applications. They may be used to detect and characterize diseases, to deliver relevant therapeutics and to study the pharmacokinetic/pharmacodynamic parameters of nanomaterials. The use of radiotracer techniques in the research of novel nanoparticles offer many advantages but there are still some limitations. The binding of radionuclides to nanoparticles has to be irreversible in order to prevent their escape to other tissues or organs. Due to the half-life of radionuclides, the manufacturing process is time-limited and difficult, and there is also a risk of contamination. This chapter present the main selection criteria for radionuclides and applicable radiolabeling procedures used for the radiolabeling of various nanoparticles. Also, an overview of different types of NPs that have so far been labeled with radionuclides is presented.

Key words: Nanoparticles; radiolabeling; nuclear imaging; radionuclide therapy; biodistribution

6.1 Introduction

Nuclear medicine is a branch of medicine that uses radiation to provide information about the functioning of a person's specific tissue/organs or to treat a disease. Radiolabeled nanoparticles (NPs) represent a new class of agents with a great potential for nuclear medicine applications. The key advantage of using radiolabeled NPs is that a very small amount can allow to obtain information of great importance [1]. They may be used to detect and characterize disease, to deliver relevant therapeutics and to monitor the therapeutic effect as well. Furthermore radiotracer-based imaging either using single-photon emission computed tomography (SPECT) or positron emission tomography (PET) is particularly suited in the study of pharmacokinetic/pharmacodynamic parameters of nanomaterials and determination of their optimal nanodimensional architecture for tissue/organ regeneration. Measuring radiation from radioactive tracers attached to nanoparticles has been demonstrated to be a highly sensitive and specific method that allows accurate quantification, without limits to tissue penetration in any organ. Nuclear imaging approaches are very suitable for detection since they offer a high detection sensitivity at high temporal and spatial resolutions requiring a radionuclide concentration of around 10^{-10} M at the site of interest.

Nanoparticulate agents typically demonstrate pharmacokinetic behavior different from that of small molecules [2] and provide flexible platforms for integration of multiple functional entities, including targeting ligands, multiple types of contrast materials and/or therapeutics. In contrast to traditional compounds used for radiopharmaceutical preparation, nanomaterials have an immense available surface area per unit of volume and tunable optical, electronic, magnetic, and biological properties. Generally, they can be tailored to meet the needs of specific applications and engineered to have different physicochemical properties that affect *in vivo* biodistribution: sizes, shapes, chemical compositions, surface chemical characteristics, and hollow or solid structures [3]. Efficient diagnosis/radiotherapy is provided

through passive targeting based on the enhanced permeability and retention (EPR) effect (Fig. 1) and/or active targeting through incorporating a targeting moiety on a nanoparticle. Non-targeted NPs can accumulate in tumors since the tumor vasculature is usually leaky and without lymphatic drainage. Active targeting is achieved by functionalizing the NPs surface with suitable vectors including peptides, antibodies and other biomolecules, which recognize characteristic epitopes at the surface of the diseased cells.

Figure 1. Passive targeting: reconstructed PET/CT imaging in Balb/c mice with ^{68}Ga-DOTA–polyamido-amine dendrimer acquired 1 h post administration; (a) the kidneys and urinary bladder in normal mice; (b) tumor uptake localized in the tumor-bearing mouse. (Reproduced with the permission of the Elsevier) [4]

Radiolabeled antibodies may effectively target even single cancer cells in circulation [5] or small cancer cell clusters [6], thereby enabling a more specific radiation dose delivery, preventing damage to healthy tissues.

6.2 Radiolabeling of nanoparticles: selection of radionuclides and optimization of the radiolabeling procedure

Several key issues need to be addressed for the selection and application of radionuclides for the radiolabeling of NPs. In contrast to NPs production, the radiolabeling process is time-limited and difficult because of the contamination risk. The handling of radionuclides has to be carried out in specially designed radiochemical laboratories with controlled ventilation and air conditioning, shielded remote handling facilities, and special equipment intended for the measuring of the radioactivity of the selected radionuclide. There are two main methods for the fabrication of radionuclides: using a nuclear reactor or using a particle accelerator. These

methods are complementary in providing a wide variety of radionuclides for the application in medicine and research (Fig. 2.).

Figure 2. Radionuclides for the radiolabeling of nanoparticles.

The ability to access radionuclides without the use of onsite accelerators or reactors depends on the availability of generator-produced radionuclides in which the parent radionuclide is produced from a reactor or cyclotron. A generator is a device that is used to extract one radionuclide from another. Molybdenum-99 (^{99}Mo)/technetium -99m (^{99m}Tc) generator is especially popular and very convenient. The differences in the half-lives and chemical properties of ^{99}Mo (half-life 66 h) and ^{99m}Tc (half-life 6 h) are exploited to separate them in the generator. This procedure can be repeated many times providing a nearly continuous supply of radionuclides at a low cost. Germanium-68/gallium-68, strontium-82/rubidium-82 and tungsten-188/rhenium-188 are newly developed generators.

The selection criteria for radionuclides must be based on the physical data about the radionuclide and biological variables governing their use. The considerations for physical characteristics include the physical half-life, type of emissions, energy of the radiation(s), daughter product (s), method of production, and radionuclide purity. The biochemical aspects include tissue targeting, the retention of radioactivity in the organ/tissue, *in vivo* stability, and toxicity.

Diagnostic radionuclides are generally short-lived radionuclides capable to provide the necessary information on biodistribution, dosimetry, and the limiting or the critical organ or the tissue. Radionuclides for SPECT imaging decay by the emission of high-energy photons (γ), while PET radionuclides decay by emission of positrons (β+). The selection of appropriate therapeutic radionuclides that emit α- or β- particles depends upon the nature, the

extent, and stage of disease. These types of particulate radiations allow very high ionisation per length of travel. Therefore, they are fully deposited within a small range of tissue (usually in mm). The longer range of beta particles can still permit uniform tumor irradiation despite a possible heterogeneity of distribution of radioactivity within the tumor. Therapeutic radionuclides which also decay with γ-radiation can be advantageous if the energy and intensity are within the diagnostic range, as it provides the ability to visualize distribution of the radiolabeled NPs [7].

The physical half-life of radionuclide plays a crucial role for measurements in the desired time frame, and it has to be considered which radionuclide or half-life, respectively, are suitable for the investigated question and pharmacokinetic profile. For measurements within a short (initial) time frame after intravenous administration, short-lived PET radionuclides have been applied, e.g., fluorine-18 (half-life 109.7 min), gallium-68 (half-life 67.7 min) or even nitrogen-13 (half-life 9.97 min) [8]. Oppositely, if the half-life is too short, most decay will occur before the radiolabeled NPs targeting has reached the maximum tissue accumulation.

The major requirements of the radiolabeling procedure are that the labeling process does not significantly alter the structure or properties of the NPs and that the stability of radiolabeled product is sufficient to allow further *in vivo* tracking. Once the radiolabeling method for the selected radionuclide and NPs type is optimized, the radioactive part may be used not only to track nanoparticles but also for radiodiagnosis or radiotherapy.

Figure 3. Radiolabeling of nanoparticles.

Depending on the radionuclide and the composition and structure of NPs, two approaches may be applied for efficient radiolabeling (Fig. 3): direct radiolabeling, mostly

via nucleophilic/electrophilic labeling and coordination chemistry, or indirect radiolabeling, via a chelator or a complexing agent, which requires additional synthetic steps. Furthermore, radionuclides are possible to attach to whole particles synthesized in advance (post-synthesis approach), or they can be entrapped in nanoparticles during the synthesis (pre-synthesis approach).

The convenience, efficiency, and gentleness of radiolabeling procedures are some of the requirements that have to be met by radiolabeling methods. The binding of radionuclides to a nanoparticle has to be irreversible in order to prevent them to escape to other tissues or organs. Careful *in vitro* experiments for measuring the stability of radiolabeled NPs (mostly in serum) are generally required prior to *in vivo* studies. The biodistribution patterns of radiolabeled nanoparticles do not seem to be crucially affected by the radiolabeling approach. In general, radiolabeled NPs are excreted into the urinary tract via the kidneys and they mostly accumulate in the reticuloendothelial tissues, liver and spleen, due to the substantial uptake by the macrophages that are present in these organs. If they agglomerate and the size is relatively large, in range of micrometers, the highest uptake after intravenous administration occurs in the lungs [9].

6.2.1 Radiolabeling with gamma-emitting radionuclides

Technetium-99m (^{99m}Tc), indium-111 (^{111}In), gallium-67 (^{67}Ga) and iodine-125 (^{125}I), are the most commonly used gamma-emitting radionuclides for NPs radiolabeling. These radionuclides emit single photons detected by a gamma camera that can view organs from many different angles.

6.2.1.1. Radiolabeling with ^{99m}Tc

Radiolabeling with ^{99m}Tc (half-life 6 h) accounts for about 80% of all nuclear medicine procedures worldwide. This can be attributed to its ideal physical properties, such as its half-life that allow for prolonged *in vivo* imaging and γ-photon single-energy emission at 140 keV,

which are beneficial for effective imaging. The chemical form of ^{99m}Tc occurs as ^{99m}Tc-pertechnetate ($^{99m}TcO_4^-$). In a chemical reaction, it is necessary to reduce its oxidation state to a lower value. Stannous chloride ($SnCl_2$) is the most often used reducing agent. The direct method of ^{99m}Tc-labeling of NPs is based on the fact that the reduced $^{99m}TcO_4$ reacts with random groups such as hydroxyl, carboxylic, amino groups, etc. present on the surface of the NPs. A direct labeling method was used to label hydroxyapatite nanoparticles (HApNP) [10], as well as astaxanthin-loaded solid lipid nanoparticles. The direct nose-to-brain delivery of the ^{99m}Tc-labeled lipid NPs was evident by gamma scintigraphy imaging, suggesting their potential use for various neurological diseases [11]. Tassano *et al.* developed another direct labeling procedure via a tricarbonyl precursor $[^{99m}Tc(H_2O)_3(CO)_3]^+$ for radiolabeling dendrimers [12]. This method has been proven to be effective for labeling various ligands, such as ethylendiamine-N,N′-diacetate, which have significant tumor uptake exclusively by passive targeting [13]. NPs loaded with these compounds have higher probability for tumor uptake.

Radiometals, both diagnostic (^{64}Cu, ^{68}Ga, ^{89}Zr) and therapeutic (^{90}Y and ^{177}Lu) are best attached to NPs via chelation. The indirect chelator-mediated ^{99m}Tc-labeling of NPs has been applied to a variety of NPs structures [14]. Helbok *et al.* performed efficient radiolabeling of PEGylated cholesterol liposomes and micelles via an acyclic diethylenetriaminepentaacetic acid (DTPA) chelator [15]. Also, PEG-liposomes can be labeled relatively easily and stably with ^{99m}Tc after liposome synthesis, using a procedure which includes the conjugation of ^{99m}Tc to hexamethyl propyleneamine (HMPAO) [16] or hydrazino nicotinamide (HYNIC) [17] followed by their encapsulation into liposomes. The HYNIC-based method provides ^{99m}Tc-labeled liposomes with a high labeling yield (>95%) and improved *in vitro* and *in vivo* characteristics compared to the liposomes labeled via ^{99m}Tc-HMPAO. Chitosan hydrogel NPs loaded with a vascular endothelial growth factor (a

potent angiogenic factor) were efficiently labeled with ^{99m}Tc via a DTPA chelator. The quantitative imaging with ^{99m}Tc-chitosan nanoparticles has been demonstrated to be a valuable strategy that can be combined with an angiogenic therapy to customize the treatment of myocardial ischemia [18]. Mercapto-acetyl-triglycine (MAG3) has been applied to facilitate radiolabeling of morpholinos [19]. *Meso*-2,3-dimercaptosuccinic acid (DMSA) is also a suitable ligand that forms complex compounds with ^{99m}Tc, ^{186}/^{188}Re,, ^{166}Ho, ^{177}Lu and ^{90}Y. DMSA enables bidentate bindinding via two sulfur atoms on silver nanoclasters (Fig. 4.) and additional radiolabeling is possible via the binding of radiometals to DMSA [20].

Figure 4. Bidentate-binding of meso-2,3-dimercaptosuccinic acid on silver nanoclusters. (Reproduced with the permission of the Elsevier) [20]

In some chelating systems it is possible to apply a theranostic approach by substituting the diagnostic radionuclide with a therapeutic one, whereas the chelator and the nanodimensional structure remain. Due to the similar chemical properties of ^{99m}Tc for ^{188}Re, the labeling procedure is based on the similar complexation chemistries of two radionuclides with the same vector.

Further studies on indirect NPs ^{99m}Tc-labeling may include the investigation of novel ligands, such as diamino dioxime ligands that form a neutral and lipophilic complex with ^{99m}Tc. The specified ligand and those that are chemically similar to it pass easily through the intact blood brain barrier. Accordingly, they have a high potential in cerebral perfusion imaging [21]. Iron oxide nanoparticles (IO-NPs) may be labeled with a variety of diagnostic and therapeutic radionuclides via direct and indirect, chelator-based radiolabeling techniques. The ^{99m}Tc-labeled aminosilane-coated IO-NPs may be promising candidates for guided cancer diagnosis and magnetic hyperthermia therapy. Targeting is enabled via the

conjugation with a new peptide-based Arg-Gly-Asp (RGD) derivate, which has a high affinity and selectivity for the αvβ3 integrin receptor presented in several tumors. The specific character of ^{99m}Tc-NPs-RGD was confirmed in a receptor blocking study, in which the co-administration of an excess amount of the native peptide blocked an experimentally induced U87MG tumor (with an over-expression of the αvβ3 receptors). This resulted in a significantly reduced uptake of ^{99m}Tc-NPs-RGD, indicating the specific character of the targeted IO-NPs (Fig.5.) [22].

Figure 5. Active targeting: representative planar γ images of ^{99m}Tc-NPs-RGD (non-blocked (A) and blocked (B)) of a U87MG tumor bearing mouse at 1h p.i. (Reproduced with the permission of the Elsevier) [22]

6.2.1.2. Radiolabeling with ^{111}In

Indium-111 (^{111}In), is a readily available gamma-emitting radiometal, which is widely used in clinical practice for diagnosis [23]. Several methods for the radiolabeling of NPs are described in the literature, involve their conjugation with a chelate. The coupling of ^{111}In to NPs can be achieved by chelating molecules like DTPA or DOTA, which are conjugated to the polymers as in the case of ^{111}In-DTPA-PEG-*b*-PCL micelles. Polyethylene glycol (PEG) is an artificial but biocompatible hydrophilic polymer that has been widely applied for NPs coating. The radiotracer method has been used to prove that it is possible to use PEG derivatives as tumor imaging carriers. After ^{111}In-labeling via DTPA, *in vivo* biodistribution studies demonstrated an increased tumor uptake and a prolonged circulation half-life with the increase of the molecular weight of PEG [24]. NPs that degrade and radionuclides that detach or are released from the NPs can cause artifacts. Dual radiolabeling using gamma emitters with different energy spectra incorporated into the core and coating may be used as a general

methodology for a wide range of engineered NPs for the visualization of the degradation process of NPs *in vivo*. In order to label the core, ^{111}In-doped iron oxide NPs were encapsulated inside poly(lactide-co-glycolide) nanoparticles (PLGA-NPs) during the preparation. The bovine serum albumin coating was labeled by electrophilic substitution using ^{125}I. Imaging revealed different fates for the core and coating, with a fraction of the two radionuclides co-localizing in the liver and lungs for long periods of time after administration, suggesting that NPs are stable in these organs [25]. The conjugation of chelating agents to nanoparticles could affect their biodistribution. The attachment of such a chelate could alter the corona of the micelles and, consequently, their biodistribution and pharmacokinetics. Similarly to other radionuclides, ^{111}In may also be entrapped in the micellar core during the formation of micelles without the need for any chemical modification [26].

Polymeric micelles (Lactosome) were labeled via 1,4,7,10-tetraazacyclododecane-1,4,7,10-tetraacetic acid (DOTA) with ^{111}In and ^{90}Y for SPECT imaging and radiotherapy, respectively. Biodistribution studies revealed that ^{111}In-DOTA-Lactosome was selectively accumulated in the tumor site of mice due to the EPR effect. The anti-tumor therapeutic effect of ^{90}Y-DOTA-Lactosome was observed depending on the dose frequency and amount [27].

6.2.1.3. Radiolabeling with ^{67}Ga

Gallium-67 (^{67}Ga) is a cyclotron-produced radiometal used for the imaging and localization of inflammatory lesions (infections). To get a better insight into the transport mechanism of peptide-conjugated NPs to tumors, bombesin (BBN) peptide-functionalized gold nanoparticles (AuNPs) were indirectly labeled with ^{67}Ga and *in vivo* biological studies of ^{67}Ga-labeled AuNPs in human prostate tumor-bearing mice were performed. In the case of ^{67}Ga, the DTPA derivatives are unable to provide a stable coordination of ^{67}Ga with AuNPs.

Therefore, ^{67}Ga-labeling was pursued via DOTA-containing AuNPs. For intravenous administration, the receptor-mediated pathway appears to be outweighed by the EPR effect while for the intraperitoneal administration, it has been concluded that the gastrin-releasing peptide receptor-mediated mechanism plays a role in pancreas uptake [28].

6.2.1.4. Radiolabeling with radioisotopes of iodine

Isotopes of iodine have been extensively used in clinical nuclear medicine imaging and radiation therapy. Out of 37 known isotopes of iodine, four - ^{123}I, ^{124}I, ^{125}I, and ^{131}I - are suitable for SPECT or PET imaging. With a 60-day half-life, γ-emitter ^{125}I is useful for the long-term tracking and imaging of radiolabeled NPs. ^{131}I (half-life 8 d) is a strong gamma emitter, but due to its mode of beta decay, it is used for beta therapy, commonly in treating thyroid cancer. Dual-purpose theranostic radionuclides, e.g. ^{131}I, or the pair ^{124}I/^{131}I can be used for imaging followed by therapy using the same radiolabeling procedure.

The traditional radiolabeling method with iodine radioisotopes is nucleophilic halogen exchange based on chloramine-T-oxidation (referred to as the Iodogen method) by direct radioiodination or by using prosthetic groups, such as tyrosine residues of proteins [29]. Tang *et al.* synthesized a SPECT/MRI/optical trimodality probe by labeling fluorescent silica-coated IO-NPs with ^{125}I using the Iodogen oxidation method. A radioactive probe was used to label mesenchymal stem cells (MSCs) and quantitatively track their migration and biodistribution in ischemic rats [30].

The radio-tracer technique has been demonstrated to be a relevant approach to the study the biodistribution of fullerenes (C_{60}). Although watersoluble C_{60} derivatives (polyhydroxylated fullerene $C_{60}(OH)_n$) were successfully radiolabeled with different radiotracers, including ^{67}Ga, ^{99m}Tc, ^{125}I or ^{14}C, similar studies have not been performed with nano C_{60}. The study of Nikolic *et al*. [31] described for the first time the efficient ^{125}I-labeling of the solvent exchange-produced C_{60} nanoparticles based on the intercalation of ^{125}I into

fullerene crystals during the colloid preparation. Fullerene molecular crystals are filled with THF molecules, but $Na^{125}I$ ion pairs are also entrapped, much more in the case when Na ^{125}I was added during than after the C_{60} dissolution (Fig. 6).

Figure 6. The proposed structure of radiolabeled C_{60} containing $Na^{125}I$ ion pair intercalated in its crystalline lattice. (Reproduced with the permission of the IOP Science) [31]

The labeling of particles after the preparation usually requires some chemical modification. HApNPs were modified with aminopropyltriethoxysilane to introduce amino groups on the surface of hydroxyapatite for effective radioiodination [32]. Labeling without any modification achieved by adding the oxidizing agent chloramine T *in situ* during the formation of HAp resulted in the reproducible high labeling yield of ^{125}I-labeled HAp [33].

6.2.2 Radiolabeling with PET radionuclides

Fluorine-18 (^{18}F, half-life 109.8 min), copper-64 (^{64}Cu half-life 12.7h), iodine-124 (^{124}I), gallium-68 (^{68}Ga, half-life 68 min) and zirconium-89 (^{89}Zr, half-life 78.4 h) are positron emitting radionuclides mostly used for PET functional imaging. Compared to SPECT imaging, PET imaging may offer increased accuracy, higher sensitivity, and better resolution [34]. PET is a more recent development in medicine and it uses radionuclides produced in a cyclotron. A cyclotron is a type of particle accelerator in which charged particles accelerate outwards from the centre along a spiral path. Limitations to the widespread use of PET arise from the high costs of cyclotrons needed to produce the short-lived radionuclides for PET scanning; the need for a specially adapted on-site chemical synthesis apparatus for radiolabeling; and a PET imaging facility in close proximity to the cyclotron due to the short half-life of most positron-emitting radionuclides. Furthermore, liposomes and some other NPs are the products of multiple steps which require a much longer process related to the half-lives of commonly used positron emitter nuclei. Thus, labeling methods in which

components of liposome or preformulated drugs are substituted with short lived positron-emitting radionuclides is impractical.

Urakami *et al*. [35] developed a rapid and efficient labeling method for lipid NPs via 1-[^{18}F] fluoro-3,6-dioxatetracosane without changing their physiological properties. Dynamic PET scanning showed that liposome-encapsulated hemoglobin (LEH) delivers oxygen even into the ischemic region from the periphery toward the core of ischemia. In recent years, the use of PET isotopes with a relatively long half-life (^{64}Cu, ^{89}Zr and ^{68}Ga) has been increased. These metals can be coupled in a straightforward fashion using chelators, such as DTPA, DOTA, 1,4,7-triazacyclononane-1,4,7-triacetic acid (NOTA), 1,4,8,11-tetraazacyclotetradecane-N,N',N'',N'''-tetraacetic acid (TETA), and derivatives of these macrocyclic chelating agents. Originally, DOTA was designed for lanthanides (e.g. Gd^{3+}), but it can be used for a wide range of radiometals as well. Since DOTA has four carboxylic functions on the side-chains of the macrocycle bearing four nitrogens, the binding of ^{64}Cu leads to deformed octahedral complexation of the Cu^{2+} ion, thereby leaving two of the acidic functions free. Accordingly, one is available for the coupling to NPs or polymers and the other allows further derivatization, or acts as an additional hydrophilic group. The review of Stockhofe *at al.* [36] presents a comprehensive study on various approaches and methods for the labeling of potential drug delivery systems using positron emitters.

^{64}Cu has favourable decay characteristics, (β^+: 0.653 MeV, 17.4%; β^-: 0.578 MeV, 39%) for both PET and radiotherapy and due to the half-life of 12.7 h it has been shown to be very effective for assessing the behaviour of nanomaterials *in vivo* for prolonged times. The functionalization of PMMA-core/PEG-shell nanoparticles with a DOTA ligand allowed for the chelation of ^{64}Cu and enabled the investigation of the biodistribution of these materials in correlation to the molecular weight of the backbone and the PEG grafts [37]. The method for ^{64}Cu-labeling via NOTA as the chelator was developed in the case of cRGD-functionalized

and doxorubicin (DOX)-conjugated IONPs for potential application in drug delivery and PET/MRI dual-modality imaging [38]. Also, the application of an improved ^{64}Cu labeling procedure via novel amine-activated chelator (amine-Bz-DOTA) conjugated to the surface of dextran sulfate coated IONPs, enabled to avoid cross-linking of IONPs (which caused NPs aggregation) and obtain a higher labeling yield [39]. Additional binding of tumor-specific antibodies to ^{64}Cu-labeled doxorubicin loaded silica-based NPs provided an increased accumulation at the tumor site via an enhanced permeability, the retention effect and antibody-mediated binding to tumor [8].

The use of ^{68}Ga (positron emission intensity 87%) is on the rise due to several identifiable properties of this radionuclide. These include a superior image quality to that provided by SPECT radionuclides and the potential for on-demand production via a generator (^{68}Ge/^{68}Ga-generator) [40]. Successful ^{68}Ga-labeling requires a chelating agent and so far, DOTA and NOTA chelators have been used to radiolabel organic and inorganic nanodimensional systems with ^{68}Ga cation. Polyamido-amine dendrimer (PAMAM) was conjugated successfully with bi-functional chelate N-hydroxysuccinimide ester of DOTA and the subsequent radiolabeling with ^{68}Ga was achieved with a high radiolabeling yield and stability. However, DOTA-like macrocycles are not the best ligands for Ga^{3+} as the incorporation of ions inside the macrocyclic cavity leads to severe distortion of the coordination octahedra around the Ga^{3+} ions. NOTA-like ligands with a bis(phosphonate)-containing side arm (as the bone targeting group) connected to a metal-binding cage through acetamide or methylphosphinate pendant arms, (NOTAM^{BP} and NO2AP^{BP}) have been shown as highly potent chelators for small $^{68}Ga^{3+}$ ions [41]. Synthetic apatite nanocrystals have demonstrated an excellent ability to bind two PET radionuclides, ^{18}F and ^{68}Ga, with a good *in vitro* stability. Na^{18}F was used for the direct incorporation of the radionuclide into the crystal

lattice, while the labeling by surface functionalization was accomplished by using ^{68}Ga-NO2AP^{BP}.

6.2.3 Radiolabeling with therapeutic β-emitting radionuclides

Currently, radionuclide therapy remains an important treatment option. The ionizing radiation from radionuclides can kill cells or inhibit the growth in the periphery and the inaccessible centers of cancerous lesions. The sites of damage comprise all cellular levels, especially DNA in the nucleus of cells [42]. Internal radiotherapy relies on the implantation of radioactive seeds, such as radiolabeled micro- and nanoparticles delivering highly localized doses to a diseased area. Due to the inhomogeneous distribution of radiolabeled particles, especially within large tumors with a necrotic center, long-range β-emitters with lower LETs and greater annihilation distances of several cells (typically 0.2-12 mm) provide a larger and tortuous radioactive dose volume. Yttrium-90 (^{90}Y), lutetium-177 (^{177}Lu) and rhenium-188 (^{188}Re) are proposed as suitable candidates for the internal radionuclide therapy, especially of primary and metastatic malignancies, while alpha- and Auger-emitters, due to their short range in tissues, would be more appropriate for the effective killing of circulating cells with a minimal irradiation of the blood [43]. No more than a few studies were conducted with α-emitting radionuclides, such as ^{225}Ac (half-life 10 d), which were mostly attached through chelation [44].

6.2.3.1 Radiolabeling with ^{90}Y

^{90}Y is a high-energy β-emitter with optimal nuclear physical characteristics (half-life 64.1 h, E_{max}=2.27 MeV) for radionuclide therapy. It can affect tumor cells up to a maximum depth of 11 mm in the soft tissue. This is described by the cross-fire effect occurring due to the long path of β-particles that crosses multiple individual cells decreasing the need for targeting each cancer cell with the radiopharmaceutical. Radiolabeled NPs, such as ^{90}Y-silicate/citrate colloid and ^{186}Re-sulfur colloid, have been used for radiosinevactomy with very encouraging

results, especially in Europe [45]. The method is based on the local intra-articular injection of nanoparticulates/colloids labeled with suitable therapeutic radionuclides into a diseased joint, where they are phagocytized by the macrophages of the inflamed synovial membrane delivering a selective radiation dose to the synovium. ^{90}Y-labeled colloid NPs, such as antimony trisulfide colloid (Sb_2S_3) [46] and tin fluoride colloid (SnF-c) [47] have a potential application in radiosinevactomy [48]. SnF-c particles were ^{90}Y-labeled by the addition of $^{90}YCl_3$ before the formation of primary particles (nucleation) and particle growth. These particles first aggregate and finally agglomerate due to the increased temperature, agitation, and aging (schematically represented in Fig. 7).The particle size of ^{90}Y-SnF-c for different therapeutic applications is controllable by manipulating the conditions under which the colloids form.

Figure 7. Formation of ^{90}Y–SnF-c agglomerates from template particles and scintigraphic images recorded at 96h after intra-articular injection in Wistar rats. (Reproduced with the permission of the Wiley) [47]

Among the different varieties of NPs proposed for use in radiosinevactomy, HAp hold considerable promise mainly due to its excellent properties [49]. Favorable properties of HAp (biocompatibility, the ease of synthesizing them within the desired particle size range, very high affinity for metal ions) have led to extensive studies on radiolabeled HApNPs with a wide variety of therapeutic radionuclides including ^{90}Y [50] ^{153}Sm [51], ^{177}Lu [52], ^{169}Er [53], ^{166}Ho [54]. The direct labeling of HApNPs has been demonstrated to be a convenient and reproducible method for the facile preparation of ^{90}Y-labeled HApNPs with a high radiolabeling yield (>98%) and radiochemical purity [55].

The direct labeling approach was also used for ^{90}Y-labeling of both Fe_3O_4-naked and Fe_3O_4-PEG600diacid NPs [56]. The carboxylate-rich surface of Fe_3O_4-PEG600diacid NPs is suitable for labeling with positively charged $^{90}Y^{3+}$. Therefore, the labeling resulted in a very high labeling yield (99%) and good *in vitro* and *in vivo* stability. Due to the significant uptake of ^{90}Y-Fe_3O_4-PEG600 NPs in liver and their low uptake by other tissues, magnetite NPs labeled with beta-emitters could be suitable for use in the combined radiotherapy-hyperthermia cancer treatment. Magnetic NPs coated with proteins, such as human serum albumin, were also effectively ^{90}Y-labeled by the direct approach without any further surface chemical modification [57]. The indirect ^{90}Y-labeling of NPs is possible via different ligands (2,3-dicarboxypropane-1,1-diphosphonic acid (DPD) (Fig. 8) [58], meso-dimercaptosuccinic acid (DMSA)) which are capable to form stable complexes with ^{90}Y.

Figure 8. Indirect ^{90}Y-labeling of NPs via DPD: the energy minimized structure of proposed complex ^{90}Y-DPD. (Reproduced with the permission of the Elsevier) [58]

6.2.3.2 Radiolabeling with ^{177}Lu

^{177}Lu (half-life 6.7 d) is the ideal β^- radionuclide for theranosis since it has a particulate emission (β^- or Auger electron) for effecting therapy and emits several accompanying gamma photons of 208 keV (11%) and 113 keV (6.4%), which are used for diagnostic evaluation and dosimetry [59]. The advantage of the long half-life of ^{177}Lu has been utilized in mapping the pharmacokinetics of potential agents, in radiosinevactomy of knee joints and the therapy of hepatocellular carcinoma. Several studies were conducted with ^{177}Lu-labeled gold NPs (AuNP) for imaging and therapy in tumor-bearing mice. AuNPs modified with PEG chains linked to DOTA made complex compounds with ^{177}Lu. Gold nanoseeds injected intratumorally were highly effective for inhibiting the growth of breast cancer tumors in CD-

1 athymic mice and caused no normal organ toxicity [60]. Targeting with ^{177}Lu-AuNPs conjugated to RGD (-Arg-Gly-Asp-) peptide showed a higher delivery into the tumor site than non-RGD and ^{177}Lu-RGD controls, highlighting the potential therapeutic capacity of radiolabeled NPs for endoradiotherapy [61]. Based on the previous work, where ^{68}Ga-labeled DOTA-conjugated bisphosphonates as PET imaging agents were investigated, a few DOTA - based bisphosphonates were synthesized and labeled with ^{177}Lu for potential application in treating metastatic bone tumors [62].

6.3 Radiolabeled NPs in nuclear medicine imaging and biodistribution studies

Different types of NPs have so far been labeled with radionuclides - from inorganic, organic to the metal and hybrid ones. Due to their good mechanical properties, chemical resistance, biocompatibility and optical and electrical properties, diamond nanoparticles (ND) represent a special research challenge in radiolabeling technologies [63, 64]. Radiolabeled diamond nanoparticles may be suitable not only for bioimaging applications, due to their stability, but they may also have wider application. Their surface enables new possibilities for functionalization, as well as the uploading of suitable proteins and drugs. ^{3}H-labeling of detonation nanodiamonds was performed by using tritium microwave (MW) plasma (Fig. 9) [65]. The analysis shows that 93% of the tritium atoms are strongly bound to the surface, while 7% are built into the ND core.

Figure 9. Tritium labeled diamond nanoparticles (ND). (Reproduced with the permission of the Royal Society of Chemistry)[65]

Exosomes are extracellular nano-sized vesicles that most cells produce. Macrophage-derived exosome-mimetic nanovesicles (ENVs) were labeled with ^{99m}Tc and their

distribution was analyzed using the SPECT/CT technique *in vivo*. The results enabled to determine the highest accumulation of ^{99m}Tc- ENVs in the liver [66].

The biodistribution of PLGA nanoparticles with and without encapsulated ascorbic acid in healthy rats was examined after their direct labeling with ^{99m}Tc, which binds outside, on the surface of nanoparticles [67]. The investigated nanospheres exhibit a prolonged blood circulation time accompanied with time-dependent reduction in the lungs, liver and spleen. This is a quick and convenient method to investigate the pharmacological behavior of a new nanoparticulate system for controlled and systemic drug delivery with a double effect [68, 69]. In such a system, it is of utmost importance to study the release of drugs from bioresorbable polymers and, in the second stage, after the resorption of the polymer, to investigate the potential of non-bioresorbable calcium phosphate as a filler in a bone defect. The surface properties of PLGA/HAp core-shell nanoparticles loaded with clindamycin and their changes under the simulated physiological conditions during the degradation process could be also investigated using radiotracer method [70].

Radiolabeled nanomaterials based on graphene, including graphene, graphene oxide (GO), reduced graphene oxide (rGO), graphene quantumdots (GQDs), and their derivatives indicate their high potential as imaging agents in a variety of bioimaging applications, especially in the PET/SPECT [71]. ^{111}In-MSN (mesoporous silica nanoparticle, MSN) proved to be suitable for the tracking of neural stem cells (NSCs) in glioblastoma therapies. Multimodal dynamic *in vivo* imaging of NSCs behavior in the brain is an important parameter in the design of a controlled, targeted and successful therapy. MSNs were labeled with ^{111}In using DOTA-NHS-ester through amide formation. SPECT confirmed the ability of ^{111}In-MSN-NSCs to penetrate through the blood brain barrier (BBB) and their localization in tumor cells [72].

Multimodality imaging by taking advantage of two or more imaging modalities can provide many structural, functional and molecular information of importance for the diagnosis and treatment [73]. It is possible to couple, e.g. MR-active NPs to a chelating system, thereby enabling *in vivo* tracking by multimodal imaging techniques (e.g. SPECT/MRI, PET/MRI). The synthesized core/shell nanoparticles of $Co_{0.16}Fe_{2.84}O_4$@$NaYF_4$(Yb, Er) and Fe_3O_4@$NaYF_4$(Yb, Tm) were stabilized with bisphosphonate polyethylene glycol conjugates (BP-PEG) and radiolabeled with ^{18}F or ^{64}Cu and ^{99m}Tc. The fabricated particles have shown the advanced features and the possibility of application in the trimodal imagining (MRI, PET/SPECT and fluorescent imaging). A high colloidal stability and a narrow size distribution (~10 nm) allow for the potential use of these particles as visual guides during surgery [74]. $^{64}Cu^{2+}$ labeled natural biopolymer based multifunctional NPs were successfully used in cancer multimodal (PET/MRI/PAI) imaging techniques [75]. "Dragon fruit-like biocage" based on apoferritin (APF) was employed (Fig. 10) to construct an efficient and excellent bio-stability nanoplatform (AMF) suitable for multimodal clinical application.

Figure 10. Schematic illustration of AMF nanocage synthesis. (Reproduced with the permission of the Elsevier) [75]

Radiolabeled ultrasmall (USNPs) nanoparticles with core sizes in the 1-3 nm range have shown specific features in biomedical applications. Due to the potential of USNPs for interactions with individual cells and the covalent attachment of small molecules, active molecular targeting can be effectively achieved [76]. ^{68}Ga-labeled iron oxide has been successfully studied using PET/MR dual-modal imaging modality during specific accumulation in tumor cells [77]. ^{65}Zn-labeled CdSe/CdS/ZnS-quantum dots (^{65}Zn-Qdots)

was used in order to achieve a full quantification of biodistribution and degradation during the *in vivo* test [78]. Depending on the attached or incorporated radioisotopes, USNPs systems have so far been mostly exploited in the SPECT and PET imaging modalities.

The particles of poorly crystalline HAp (d50=72 nm) coated with chitosan (Ch), and the chitosan-poly-D,L-lactide-co-glycolide polymer blend (Ch-PLGA) have shown multi-functional characteristics in bone tissue engineering [79]. ^{125}I was used for the *in situ* radiolabeling of HAp, HAp/Ch and HAp/Ch-PLGA synthesized particles. Biodistribution studies have shown that after the intravenous administration to normal male Wistar rats, HAp particles have the highest liver accumulation 10 min after injection and rapid excretion from the body without residual radioactivity 24 hours after injection [33]. HAp/Ch particles have the highest accumulation in the liver 10 min after injection with considerable amount (almost 50 %) retained 24 hours later. HAp/Ch-PLGA has the highest uptake in the lungs 10 minutes after injection and moderate retention in the same organ 24 hours later (Fig. 11). The results of the biodistribution of ^{125}I-labeled particles based on HAp NPs indicate that they could be applied as organ-targeting carriers of various drugs in therapy.

Figure 11. Biodistribution of a) ^{125}I-HAp , b) ^{125}I-HAp/Ch and c) ^{125}I-HAp/Ch-PLGA. (Reproduced with the permission of the Elsevier) [33]

Different approaches to the radiolabeling of super paramagnetic iron oxide nanoparticles (SPIONs) with ^{14}C were tested in order to obtain a suitable system that could be used in the analysis of biodistribution. The concept of surface functionalization and formation of a multiple core system made it possible to obtain particles with a hydrodynamic radius smaller than 100 nm. NPs are functionalized with polycarboxylate or polyamine surface functional groups and ^{14}C is incorporated directly into the carbon backbone of the organic

molecules. This concept make is possible to obtain identical surface chemical functionality of labeled and non-labeled particles, enabling an accurate analysis prior to potential clinical application [80]. Nanoparticle carrier crown-ether-conjugated silica (SiNPs) is radiolabeled with ^{22}Na with a loading efficacy of 98.1%±1.4%. Due to the relatively long half-life of 2.6 years, this radionuclide has not had a wider application in biomedicine. However, for these reasons, ^{22}Na may represent a practical choice in research. The one-month *in vivo* study on Female Balb/c mice (six weeks old) showed that ^{22}Na-SiNPs were removed from the organism after two weeks, and completely after a month. The highest accumulation of particles was recorded in the liver 5 min. after intravenous administration [81]. Heat-induced metal ion binding reaction, which enables radiolabeling without modifying the surface structure, was used for the labeling of paramagnetic iron oxide nanoparticles. Feraheme (FH, solution composed of a non-stoichiometric Fe_3O_4 magnetite core approximately 5–10 nm in diameter stabilized with a carboxymethyl dextran coating; total size: 17-31 nm in diameter) NPs were labeled with ^{89}Zr in a thermal reaction at 120°C in less than 60 minutes. The biodistribution of ^{89}Zr-FHNPs 96h after the intravenous injection to mice indicated the uptake of ^{89}Zr–FH in the lymphatic system [82].

In order to analyze and interpret the biodistribution of various components of multi-component and more complex nano systems the concept of dual-radiolabeling of NPs was applied. Citrate-coated gold nanoparticles (monodisperse, 14 nm in diameter) were labeled with ^{14}C and ^{198}Au. By using liquid scintillation to determine ^{14}C and gamma spectroscopy for ^{198}Au different biodistribution profiles were determined for the Au core and the citrate surface coating over time. The obtained results of biodistribution show that over time the delamination and degradation of the citrate coating of NPs occur [83]. PLGA-coated iron oxide NPs were labeled with two gamma emitters ^{111}In and ^{125}I (Fig. 12) in the way that during the synthesis Au was labeled with ^{111}In and PLGA with ^{125}I. The energy-discriminant

SPECT modality was used to analyze each radioisotope independently during the *in vivo* test with mice (BALB/cJRJ). The results showed that over time, the PLGA surface coating separated from the core since ^{125}I was detected in the thyroid glands and urine, and ^{111}In in the liver [25].

Figure 12. Schematic representation of dual-labeled [$^{125}I/^{111}In$] of PLGA-coated iron oxide NPs. (Source: J. Llop, et al., (2015)) [25]

6.6 Radiolabeled NPs in therapy

New research strategies in designing radiolabeled NPs are aimed at obtaining radiolabeled multifunctional nano objects that would accomplish specific and targeted therapy [84, 85]. Functional nanoparticles with active targeting (targeted nanoparticles, TNPs) could serve as carriers of radionuclides in the radio therapy of cancer with a high mortality of cancer cells while simultaneously sparing normal cells with minimal side effects [86]. HAp NPs radiolabeled with ^{99m}Tc have shown a high stability during *in vivo* studies in mice. The results showed a higher affinity to bone tissues in contrast to the surrounding muscle tissue [87].

In order to achieve a more specific targeting, TNPs are functionalized with various molecules. Anti-cancer therapeutic properties of the ^{125}I labeled hybrid nano-sized cyclic Arg-Gly-Asp-conjugated GoldNPs (cRGD-GNPs) system were tested (including acute apoptosis two days post treatment and long-term influence up to 21 days). The results confirmed the effective targeting of tumor with ^{125}I-cRGD-GNP and the suppression of its growth [88]. It has been demonstrated that the systems based on gold nanoparticles (GNPs) functionalized with an epidermal growth factor (EGF) as carriers of ^{111}In are successful in the targeting and therapy of EGF receptor-positive cancers [89]. Targeted radiotherapy was also

successfully achieved with conjugated surfaces of nano-systems on the basis of BSA (Bovine serum albumin) nanocapsules, silica, monoclonal antibodies (mAbs), etc [90-92].

Multifunctional nanoplatforms for the simultaneous use of radiotherapy and chemotherapy could enable significant progress in the field of nano-oncology. The designed lipid-polymer hybrid nanoplatform ChemoRad (Fig. 13), which contains PLGA and lecithin, was used as a suitable carrier for docetaxel, ^{111}In and ^{90}Y [93]. The results obtained with the prostate cancer model confirmed the realization of highly specific targeted delivery of the drug with highly effective radiotherapy at the same time.

Figure 13. Schematic representation of the ChemoRad NPs. (Reproduced with the permission of the Elsevier) [94]

6.7 Radiolabeled NPs in theranostics

Multifunctional nanoparticulate systems with hybrid and improved properties are a result of creative research. Clear boundaries between objects for diagnostic imaging, therapy or biodistribution have almost disappeared. The term "theranostics" has unified the diagnostic and therapeutic potentials of the system into a single agent in order to achieve efficient, specific and individual therapy in various diseases [95].

Gadolinium-doped hydroxyapatite (HAp-Gd) nanorods could be used as theranostic nanoparticles to detect the early stages of osteosarcoma, or as carriers of radioisotopes in therapy. Gadolinium endows HAp with paramagnetic properties, while phosphorous and gadolinium in the HAp-Gd sample can be activated by neutron capture, in a nuclear reactor, producing ^{32}P and ^{159}Gd radioisotopes [96]. The multifunctional platform based on single-walled carbon nanotubes (SWNTs) coated with a shell of polydopamine (PDA) was modified with polyethylene glycol (PEG). SWNT@PDA-PEG was labeled with ^{131}I nucleotide, which

potentially allows nuclear imaging and cancer therapy. An *in vivo* study in mice confirmed the accumulation of intravenously administered ^{131}I-SWNT@PDA-PEG in the tumor tissues. The PDA coating allowed an easy labeling with ^{131}I but also its delivery, due to which the system was able to perform radionuclide therapy as well [97].

A particular research challenge is focused on the preparation of radiolabeled nanoparticles with significant *in vivo* stability. A detailed analysis of the chelator-free radio-labeling technique indicates the vital importance of deprotonated silanol groups during the labeling of mesoporous (MSN) (Fig. 14a) and nonporous (dSiO2) silica nanoparticles (Fig. 14b) with ^{89}Zr in order to obtain long stable systems. The *in vivo* study of the stability of these systems indicates that the detachment rate of ^{89}Zr-MSN is about 20 times slower than that of ^{89}Zr-dSiO_2. The results obtained with PET modality indicated that the existence of mesochannels within MSN particles is responsible for the high stability of ^{89}Zr-MSN system over a period of three weeks [98]. After the injection of ^{89}Zr-MSN, their accumulation in the liver and spleen can be perceived, while the bone uptake is not present, which is not the case with ^{89}Zr-dSiO_2.

Figure 14. ^{89}Zr-labeled silica nanoparticles: a) mesoporous (MSN) and b) nonporous (dSiO2). (Adapted and reprinted with the permission of the American Chemical Society Publications) [98]

A long circulation half-life of in vivo radiolabeled NPs leaves enough time for the EPR effect and the successful implementation of this type of particles in theragnostics. The ^{64}Cu-labeled PEGylated reduced graphene oxide-iron oxide nanoparticles (^{64}Cu-PEGylated RGO-IONPs) reaching about 68 nm in size were intravenously administered to mice which had an ischemic hind limb. On the basis of positron emission tomography (PET) and Doppler

imaging it was determined that the accumulation of particles in the ischemic hind limb was the highest after three days and the lowest after 17 days [99].

References

[1] D. Soo Lee, H.J. Im, Y.S. Lee, Radionanomedicine: Widened perspectives of molecular theragnosis, Nanomedicine 11 (2015) 795-810.

[2] S. Vranješ, M.S. Jovanović, M. Prvulović, Lj. Stefanović, R. Kljajić, R. Ratajac, Chemical and biological properties of verapamil labeled with technetium-99m-potential myocardial imaging agents, J. Radioanal. Nucl. Chem. 253 (2002) 81-86.

[3] A.L.B. de Barros, A. Tsourkas, B. Saboury, V. Nascimento Cardoso, A. Alavi, Emerging role of radiolabeled nanoparticles as an effective diagnostic technique, EJNMMI Res. 2 (2012) 39.

[4] A. Ghai, B. Singh, P. Panwar Hazari, M.K. Schultz, A. Parmar, P. Kumar, et al., Radiolabeling optimization and characterization of 68Galabeled DOTA-polyamido-amine dendrimer conjugate - Animal biodistribution and PET imaging results, Appl Radiat Isot. 105 (2015) 40-46.

[5] G.-J. Beyer, M. Miederer, S. Vranješ-Đurić, J.J. Čomor, G. Kuenzi, O. Hartley, et al., Targeted alpha therapy in vivo: direct evidence for single cancer cell kill using 149Tb-Rituximab, Eur. J. Nucl. Med. Mol. Imag. 1 (4) (2004) 547-554.

[6] M. Fani, S. Vranješ, S.C. Archimandritis, S. Potamianos, S. Xanthopoulos, P. Bouziotis, et al., Labelling of monoclonal antibodies with samarium-153 for potential use in radioimmunotherapy, App. Radiat. Isot. 57 (2002) 665-674.

[7] C.-H. Yeong, M.H. Cheng, K.H. Ng, Therapeutic radionuclides in nuclear medicine:current and future prospects, J. Zhejiang. Univ. Sci. B. 15 (10) (2014) 845-863.

[8] K. Stockhofe, J.M. Postema, H. Schieferstein, T.L. Ross, Radiolabeling of Nanoparticles and Polymers for PET Imaging, Pharmaceuticals (Basel). 7 (2014) 392-418.

[9] S.C. Srivastava, L.F. Mausner, Therapeutic Radionuclides: Production, physical characteristics, and applications, in: R.P. Baum (Ed.), Therapeutic nuclear medicine, medical radiology. Radiation Oncology, Springer-Verlag Berlin Heidelberg, 2013, pp 11-41.

[10] A.L. Maia, C.H. Cavalcante, M.G. De Souza, A.F. De Carolina, D. Rubello, S. Chondrogiannis, et al., Hydroxyapatite nanoparticles: Preparation, characterization, and evaluation of their potential use in bone targeting: An animal study, Nucl Med Commun., 37 (2016) 775-782.

[11] C. Bhatt, P. Srivastava, P. Pandey, P. Khan, W. Panda, Nose to brain delivery of astaxanthin¬loaded solid lipid nanoparticles: Fabrication, radio labeling, optimization and biological studies, RSC Adv. 6 (2016) 10001-10010.

[12] M.R. Tassano, P.F. Audicio, J.P. Gambini, M. Fernandez, J.P. Damian, M. Moreno, et al., Development of 99mTc$(CO)_3$-dendrimer-FITC for cancer imaging, Bioorg. Med. Chem. Lett. 21 (2011) 5598–5601.

[13] M. Lakić, Lj. Sabo, S. Ristić, A. Savić, S. Petričević, N. Nikolić, et al., Synthesis and biological evaluation of 99mTc-tricarbonyl complex of O,O`-diethyl ethylenediamine-N,N´-di-3-propanoate as potential tumor diagnostic agents, Appl. Organomet. Chem. 30 (2016) 81-88.

[14] D. Psimadas, P. Bouziotis, P. Georgoulias, V. Valotassiou, T. Tsotakos, G. Loudos, Radiolabeling approaches of nanoparticles with 99mTc, Contrast Media Mol. Imaging 8 (2013) 333–339.

[15] A. Helbok, C. Decristoforo, G. Dobrozemsky, C. Rangger, E. Diederen, B. Stark, et al., Radiolabeling of lipid-based nanoparticles for diagnostics and therapeutic applications: a comparison using different radiometals, J. Liposome Res. 20 (2010) 219-227.

[16] E.T.M. Dams, W.J.G. Oyen, O.C. Boerman, G. Storm, P. Laverman, P.J.M. Kok, et al., 99mTc PEG Liposomes for the scintigraphic detection of infection and inflammation: Clinical evaluation, J Nucl Med. 41 (2000) 622-630.

[17] P. Laverman, E.T.M. Dams, W.J.G. Oyen, G. Storm, E.B. Koenders, R. Prevost, et al., A novel method to label liposomes with Tc-99m via the hydrazino nicotinyl derivative, J. Nucl. Med. 40 (l999) 192-197.

[18] H. Hwang, J. Kwon, P.S. Oh, T.K. Lee, K.S. Na, C.M. Lee, et al., Peptide-loaded nanoparticles and radionuclide imaging for individualized treatment of myocardial ischemia, Radiology 273 (2014) 160-167.

[19] B.L. Faintuch, G.E. Núñez, R. Teodoro, A.M. Moro, J. Mengatti, Radiolabeled nano-peptides show specificity for an animal model of human PC3 prostate cancer cells, Clinics 66 (2011) 327-336.

[20] O. Zaluzhna, L. Brightful, T.C.Allison, Y.J. Tong, Spectroscopic evidence of a bidentate-binding of meso-2,3-dimercaptosuccinic acid on silver nanoclusters, Chem. Phys. Lett. 509 (2011) 148-151.

[21] M. Mirković, D. Janković, S. Vranješ-Đurić, M. Radović, D. Stanković, D. Mijin, et al., Novel tetradentate diamine dioxime ligands: synthesis, characterization and in vivo behavior of their 99mTc-complexes, Appl. Organomet. Chem. 26 (2012) 347-355.

[22] I. Tsiapa, E.K. Efthimiadou, E. Fragogeorgi, G. Loudos, A.D. Varvarigou, P. Bouziotis, et al., 99mTc-labeled aminosilane-coated iron oxide nanoparticles for molecular imaging of $\alpha_v\beta_3$-mediated tumor expression and feasibility for hyperthermia treatment, J. Colloid Interface Sci. 433 (2014) 163-175.

[23] D. Psimadas, P. Georgoulias, V. Valotassiou, G. Loudos, Molecular nanomedicine towards cancer: ^{111}In-labeled nanoparticles, J. Pharm, Sci, 101 (2012) 2271-2280.

[24] K. Kanazaki, K. Sano, A. Makino, F. Yamauchi, A. Takahashi, T. Homma, et al., Feasibility of poly(ethylene glycol) derivatives as diagnostic drug carriers for tumor imaging, J. Control. Release 226 (2016) 115-123.

[25] J. Llop, P. Jiang, M. Marradi, V. Gómez-Vallejo, M. Echeverría, S. Yu, et al., Visualisation of dual radiolabelled poly(lactide-co-glycolide) nanoparticle degradation in vivo using energy discriminant SPECT, J. Mater. Chem. B, 3 (2015) 6293-6300.

[26] A.C. Laan, C. Santini, L. Jennings, M.de Jong, M.R. Bernsen, A.G. Denkova, Radiolabeling polymeric micelles for in vivo evaluation: a novel, fast, and facile method, EJNMMI Research 6 (2016) 1-10.

[27] K. Kurihara, M. Ueda, I. Hara, E. Hara, K. Sano, A. Makino, et al., Inflammation-induced synergetic enhancement of nanoparticle treatments with DOXIL® and ^{90}Y-Lactosome for orthotopic mammary tumor, J. Nanopart. Res. 18 (2016) 137.

[28] F. Silva, A. Zambre, M.P.C. Campello, L. Gano, I. Santos, A.M. Ferraria, et al., Interrogating the role of receptor-mediated mechanisms: biological fate of peptide-functionalized radiolabeled gold nanoparticles in tumor mice, Bioconjug. Chem. 27 (2016) 1153-1164.

[29] M. Benezra, O. Penate-Medina, P.B. Zanzonico, D. Schaer, H. Ow, A. Burns, et al., Multimodal silica nanoparticles are effective cancer-targeted probes in a model of human melanoma, J. Clin. Invest. 121 (2011) 2768-2780.

[30] Y. Tang, C. Zhang, J. Wang, X. Lin, L. Zhang, Y. Yang, et al., MRI/SPECT/fluorescent tri-modal probe for evaluating the homing and therapeutic efficacy of transplanted mesenchymal stem cells in a rat ischemic stroke model, Adv. Funct. Mater. 25 (2015) 1024-1034.

[31] N. Nikolić, S. Vranjes-Đurić, D. Janković, D. Đokić, M. Mirković, N. Bibić, et al., Preparation and biodistribution of radiolabeled fullerene C60 nanocrystals, Nanotechnology 20 (2009) 385102-385109.

[32] G.P. Xie, W.X. Lu, In vivo tissue distribution of hydroxyapatite nanoparticles modified with aminopropyltriethoxysilane, Chinese Pharm. J. 50 (8) (2015) 695-699.

[33] N. Ignjatović, S. Vranješ Đurić, Ž. Mitić, D. Janković, D. Uskoković, Investigating an organ-targeting platform based on hydroxyapatite nanoparticles using a novel in situ method of radioactive 125Iodine labeling, Mater. Sci. Eng. C Mater. Biol. Appl. 43 (2014) 439-446.

[34] F. Ai, C.A. Ferreira, F. Chen, W. Cai, Engineering of radiolabeled iron oxide nanoparticles for dual modality imaging, Wiley Interdiscip. Rev. Nanomed. Nanobiotechnol. 8 (2016) 619-630.

[35] T. Urakami, A.T. Kawaguchi, S. Akai, K. Hatanaka, H. Koide, K. Shimizu, et al., In vivo distribution of liposome¬encapsulated hemoglobin determined by positron emission tomography, Artif. Organs 33 (2009) 164-168.

[36] K. Stockhofe, J. M. Postema, H. Schieferstein, T.L. Ross, Radiolabeling of Nanoparticles and Polymers for PET Imaging, Pharmaceuticals 7 (2014) 392-418.

[37] E.D. Pressly, R. Rossin, A. Hagooly, K. Fukukawa, B.W. Messmore, M.J. Welch, et al., Structural effects on the biodistribution and positron emission nanoparticles comprised of amphiphilic block graft copolymers, Biomacromolecules 8 (2007) 3126-3134.

[38] X. Yang, H. Hong, J.J. Grailer, I.J. Rowland, A. Javadi, S.A. Hurley, et al., cRGD-functionalized, DOX-conjugated, and Cu-labeled superparamagnetic iron oxide nanoparticlesfor targeted anticancer drug delivery and PET/MR imaging, Biomaterials 32 (2011) 4151-4160.

[39] B.R. Jarrett, B. Gustafsson, D.L. Kukis, A.Y. Louie, Synthesis of ^{64}Cu-labeled magnetic nanoparticles for multimodal imaging, Bioconjug. Chem. 19 (2008)1496–1504.

[40] F. Rösch, P.J. Riss, The renaissance of the 68Ge/68Ga radionuclide generator initiates new developments in 68Ga radiopharmaceutical chemistry, Curr. Top Med. Chem. 10 (2010) 1633-1668.

[41] J. Holub, M. Meckel, V. Kubíček, F. Rösch, P. Hermann, Gallium(III) complexes of NOTA-bis (phosphonate) conjugates as PET radiotracers for bone imaging, Contrast Media Mol. Imaging, 10 (2015) 122-134.

[42] E. Morales-Avila, M. Ortiz-Reynoso, M. Seyedeh Fatemeh, A. Amirhossein, Multifunctional radiolabeled nanoparticles: strategies and novel classification of radiopharmaceuticals for cancer treatment, J. Drug Target. 23 (2015) 191-201.

[43] G.J. Beyer, J.J. Čomor, M. Daković, D. Soloviev, C. Tamburella, E. Hageb, et al., Production routes of the alpha emitting 149-Tb for medical application, Radiochim. Acta 90 (2002) 247-252.

[44] M.F. McLaughlin, J. Woodward, R.A. Boll, J.S. Wall, A.J. Rondinone, S.J. Kennel, et al. Gold coated lanthanide phosphate nanoparticlesfor targeted alpha generator radiotherapy, PLoS One 8 (2013) 2-9.

[45] F.F.R. Knapp, A. Dash, Radiopharmaceuticals for therapy, in: Radiopharmaceuticals for Therapy, Springer India, 2016, pp. 1-347.

[46] D. Janković, T. Maksin, D. Đokić, S. Milonjić, N. Nikolić, M. Mirković, et al., Particle size analysiss: 90Y and 99mTc-labelled colloids, J. Microsc. 232 (2008) 601-604.

[47] D. Jankovic, S. Vranjes-Djuric, D. Djokic, M. Markovic, B. Ajdinovic, Lj. Jaukovic, et al., 90Y-labeled tin fluoride colloid as a promising therapeutic agent: preparation, characterization, and biological study in rats, J. Pharm. Sci. 101 (2012) 2194-2203.

[48] F.M. van der Zant, R.O. Boer, J.D. Moolenberg, Z.N. Jahangier, J.W.J. Bijlsma, J.W.G. Jacobs, Radiation synovectomy with 90Yttrium, 186Rhenium and 169Erbium: a systematic literature review and meta-analysis, Clin. Exp. Rheumatol. 27 (2009) 130-139.

[49] S. Chakraborty, K.V. Vimalnath, A. Rajeswari, A. Shinto, E.R. Radhakrishnan, A. Dash, Radiolanthanide-labeled HA particles in the treatment of rheumatoid arthritis: ready-to-use cold kits for rapid formulation in hospital radiopharmacy, J. Radioanal. Nucl. Chem. 302 (2014) 875-881.

[50] W.U. Kampen, M. Voth, J. Pinkert, A. Krause, Therapeutic status of radiosynoviorthesis of the knee with yttrium [90Y] colloid in rheumatoid arthritis and related indications, Rheumatology, 46 (2007) 16-24.

[51] M. Chinol, S. Vallabhajosula, S.J. Goldsmith, M.J. Klein, K.F. Deutsch, L.K. Chinen, et al., Chemistry and biological behaviour of Samarium-153 and Rhenium-186-labeled hydroxyapatite particles: potential radiopharmaceuticals for radiation synovectomy, J. Nucl. Med. 34 (1993) 1536-1542.

[52] S. Chakraborty, T. Das, S. Banerjee, H.D. Sarma, M. Venkatesh, Preparation and preliminary biological evaluation of 177Lu labeled hydroxyapatite as a promising agent for radiation synovectomy of small joints, Nuc.l Med. Commun. 27 (2006), 661-668.

[53] S. Chakraborty, T. Das, V. Chirayil, S.P. Lohar, H.D. Sharma, Erbium-169 labeled hydroxyapatite particulates for use in radiation synovectomy of digital joints-a preliminary investigation, Radiochim. Acta. 102 (2014) 443-450.

[54] P.R. Unni, P.R. Chaudhari, M. Venkatesh, N. Ramamoorthy, M.R.A. Pillai, Prepration and bioevaluation of 166Ho labeled hydroxyapatite (HA) particles for radiosynovectomy, Nucl. Med. Biol. 29 (2002) 199-209.

[55] K.V. Vimalnath, S. Chakraborty, A. Rajeswari, H.D. Sarma, J. Nuwad, U. Pandey, et al., Radiochemistry, pre-clinical studies and first clinical investigation of 90Y-labeled hydroxyapatite (HA) particles prepared utilizing 90Y produced by (n,γ) route, Nuc. Med. Biol. 42 (2015) 455-464.

[56] M. Radovic, M.P. Calatayud, G.F. Goya, M.R. Ibarra, B. Antic, V. Spasojevic, et al., Preparation and in vivo evaluation of multifunctional 90Y-labeled magnetic nanoparticles designed for cancer therap, J. Biomed. Mater. Res. A 103 (2015) 126-134.

[57] M. Radović, S. Vranješ-Đurić, N. Nikolić, D. Janković, G. F. Goya, T. Torres, et al., Development and evaluation of 90Y-labeled albumin microspheres loaded with magnetite nanoparticles for possible applications in cancer therapy, J. Mat. Chem. 22 (2012) 24017-24025.

[58] D.Dj. Djokić, D.Lj. Janković, N.S. Nikolić, Labeling, characterization, and in vivo localization of a new 90Y-based phosphonate chelate 2,3-dicarboxypropane-1,1-diphosphonic acid for the treatment of bone metastases: Comparison with 99mTc- DPD complex, Bioorg. Med. Chem. 16 (2008) 4457-4465.

[59] S. Banerjee, T. Das, Theranostic, Applications of Lutetium-177 in Radionuclide Therapy, Curr. Radiopharm. 9 (2016) 94-101.

[60] S. Yook, Z. Cai, Y. Lu, M.A. Winnik, J.P. Pignol, R.M. Reilly, Intratumorally injected ^{177}Lu-labeled gold nanoparticles: Gold nanoseed brachytherapy with application for neoadjuvant treatment of locally advanced breast cancer, J. Nucl. Med. 57 (2016) 936-942

[61] A. Vilchis-Juárez, G. Ferro-Flores, C. Santos-Cuevas, E. Morales-Avila, B. Ocampo-García, L. Díaz-Nieto, et al., Molecular targeting radiotherapy with Cyclo-RGDfK(C) peptides conjugated to 177Lu-labeled gold nanoparticles in tumor-bearing mice, J. Biomed. Nanotechnol. 10 (2014) 393-404.

[62] R. Bergmann, M. Meckel, V. Kubíček, J. Pietzsch, J. Steinbach, P. Hermann, et al., 177Lu-labelled macrocyclic bisphosphonates for targeting bone metastasis in cancer treatment, EJNMMI Research 6 (2016) 1-12.

[63] D. Ho, C.-H.K. Wang, E.K.-H. Chow, Nanodiamonds: The intersection of nanotechnology, drug development, and personalized medicine, Sci. Adv. 1 (2015) e1500439.

[64] V.N. Mochalin, O. Shenderova, D. Ho, Y. Gogotsi, The properties and applications of nanodiamonds, Nat. Nanotechnol. 7 (2012) 11-23.

[65] H. Girard, A. El-Charbachi, S. Garcia-Arqote, T. Petit, P. Bergonzo, B. Rousseau, et al., Tritium labeling of detonation nanodiamonds, Chem. Commun. 50 (2014) 2916-2918.

[66] H.D. Won, C. Hongyoon, J.S. Chul, Y.Y. Min, P.J. Yong, C.N. Eun, et al., Noninvasive imaging of radiolabeled exosome-mimetic nanovesicle using ^{99m}Tc-HMPAO, Sci. Rep. 5 (2015) 15636.

[67] M. Stevanović, T. Maksin, J. Petković, M. Filipic, D. Uskoković, An innovative, quick and convenient labeling method for the investigation of pharmacological behavior and the metabolism of poly(DL-lactide-co-glycolide) nanospheres, Nanotechnology 20 (2009) 335102.

[68] N.L. Ignjatović, P. Ninkov, R. Sabetrasekh, D.P. Uskoković, A novel nano drug delivery system based on tigecycline-loaded calcium phosphate coated with poly-DL-lactide-co-glycolide, J. Mater. Sci. Mater. Med. 21 (2010) 231-239.

[69] N. Ignjatović, V. Uskoković, Z. Ajduković, D. Uskoković, Multifunctional hydroxyapatite and poly(d,l-lactide-co-glycolide) nanoparticles for the local delivery of cholecalciferol, Mater. Sci. Eng. C Mater. Biol. Appl. 33 (2013) 943-950.

[70] M. Vukomanović, I. Šarčev, B. Petronijević, S. D. Škapin, N. Ignjatović, D. Uskoković, Poly(d,l-lactide-co-glycolide)/hydroxyapatite core-shell nanospheres. Part 4: A change of the surface properties during degradation process and the corresponding in vitro cellular response, Colloid. Surface B 91 (2012) 144-153.

[71] J. Lin, X. Huang, Graphene-based nanomaterials for bioimaging, Adv. Drug Deliv. Rev. 105 (2016) 242-254.

[72] S.-H. Cheng, D. Yu, H.-M. Tsai, R. Morshed, D. Kanojia, L.-W. Lo, et al., Dynamic in vivo SPECT imaging of neural stem cells functionalized with radiolabeled nanoparticles for tracking of glioblastoma, J. Nucl. Med. 57 (2016) 279-284.

[73] Y. Xing, J. Zhao, P. Conti, K. Chen, Radiolabeled nanoparticles for multimodality tumor imaging, Theranostics 4 (2014) 290-305.

[74] X. Cui, D. Mathe, N. Kovács, I. Horváth, M. Jauregui-Osoro, R. Torres Martin de Rosales, et al., Synthesis, characterization, and application of core–shell $Co_{0.16}Fe_{2.84}O_4$@$NaYF_4$(Yb, Er) and Fe_3O_4@$NaYF_4$(Yb, Tm) nanoparticle as trimodal (MRI, PET/SPECT, and optical) imaging agents, Bioconjug. Chem. 27 (2016) 319-328.

[75] M.Yang, Q. Fan, R. Zhang, K. Cheng, J. Yan, D. Pan, et al., Dragon fruit-like biocage as an iron trapping nanoplatform for high efficiency targeted cancer multimodality imaging, Biomaterials 69 (2015) 30-37.

[76] K. Zarschler, L. Rocks, N. Licciardello, L. Boselli, E. Polo, K. Pombo Garcia, et al., Ultrasmall inorganic nanoparticles: State-of-the-art and perspectives for biomedical applications, Nanomedicine 12 (2016) 1663-1701.

[77] S.H. Moon, B.Y. Yang, Y.J. Kim, M.K. Hong, Y.S. Lee, D.S. Lee, et al. Development of a complementary PET/MR dual-modal imaging probe for targeting prostate-specific membrane antigen (PSMA), Nanomedicine 12 (2016) 871-879.

[78] D. Bargheer, A. Giemsa, B. Freund, M. Heine, C. Waurisch, G.M. Stachowski, et al., The distribution and degradation of radiolabeled superparamagnetic iron oxide nanoparticles and quantum dots in mice, Beilstein J. Nanotechnol. 6 (2015) 111-123.

[79] N. Ignjatović, V. Wu, Z. Ajduković, T. Mihajilov-Krstev, V. Uskoković and D. Uskoković, Chitosan-PLGA polymer blends as coatings for hydroxyapatite nanoparticles and

their effect on antimicrobial properties, osteoconductivity and regeneration of osseous tissues, Mater. Sci. Eng. C Mater. Biol. Appl. 60 (2016) 357-364.

[80] P. Nallathamby, N. Mortensen, H. Palko, M. Malfatti, C. Smith, J. Sonnett, et al., New surface radiolabeling schemes of super paramagnetic iron oxide nanoparticles (SPIONs) for biodistribution studies, Nanoscale 7 (2015) 6545-6555.

[81] A. Al Faraj, B. Alotaibi, A. P. Shaik, K.Z Shamma, I. Al Jammaz, J. Gerl, Sodium-22-radiolabeled silica nanoparticles as new radiotracer for biomedical applications: in vivo positron emission tomography imaging, biodistribution, and biocompatibility, Int. J. Nanomedicine 10 (2015) 6293-6302.

[82] E. Boros, A. Bowen, L. Josephson, N. Vasdev, J. Holland, Chelate-free metal ion binding and heat-induced radiolabeling of iron oxide nanoparticles, Chem. Sci. 6 (2015) 225-236.

[83] C. Rambanapasi, N. Barnard, A. Grobler, H. Buntting, M. Sonopo, D. Jansen, et al., Dual radiolabeling as a technique to track nanocarriers: The case of gold nanoparticles, Molecules 20 (2015) 12863-12879.

[84] M.K. Yu, J. Park, S. Jon, Targeting strategies for multifunctional nanoparticles in cancer imaging and therapy, Theranostics 2 (2012) 3-44.

[85] J. Koziorowski, A. Stanciu, V. Gómez-Vallejo, J. Llop, Radiolabeled nanoparticles for cancer diagnosis and therapy, Anticancer Agents Med. Chem. 2016 [E-pub ahead of print], http://dx.doi.org/10.2174/1871520616666160219162902

[86] K.T. Nguyen, Targeted nanoparticles for cancer therapy: Promises and challenges, J. Nanomedic. Nanotechnol. 2 (2011) 103e.

[87] A.L. Maia, C.H. Cavalcante, M.G. Souza, C.deA. Ferreira, D. Rubello, S. Chondrogiannis, et al., Hydroxyapatite nanoparticles: preparation, characterization, and

evaluation of their potential use in bone targeting: an animal study, Nucl. Med. Commun. 37 (2016) 775-782.

[88] N. Su, Y. Dang, G. Liang, G. Liu, Iodine-125-labeled cRGD-gold nanoparticles as tumor-targeted radiosensitizer and imaging agent, Nanoscale Res. Lett. 10 (2015) 160.

[89] L. Song, N. Falzone, K.A. Vallis, EGF-coated gold nanoparticles provide an efficient nano-scale delivery system for the molecular radiotherapy of EGFR-positive cancer, Int. J. Radiat. Biol. 2016 [E-pub ahead of print], http://dx.doi.org/10.3109/09553002.2016.1145360

[90] S. Liang, X. Jin, Y. Ma, J. Guo, H. Wang, Folic acid-conjugated BSA nanocapsule (n-BSA-FA) for cancer targeted radiotherapy and imaging, RSC Advances 5 (2015) 88560-88566.

[91] F. Chen, H. Hong, Y. Zhang, H. Valdovinos, S. Shi, G. Kwon, et al., In vivo tumor targeting and image-guided drug delivery with antibody-conjugated, radio labeled mesoporous silica nanoparticles, ACS Nano 7 (2013) 9027-9039.

[92] A. Scott, J. Wolchok, L. Old, Antibody therapy of cancer, Nat. Rev. Cancer 12 (2012) 278-287.

[93] A. Wang, K. Yuet, L. Zhang, F. Gu, M. Huynh-Le, A. Radovic-Moreno, et al., ChemoRad nanoparticles: a novel multifunctional nanoparticle platform for targeted delivery of concurrent chemoradiation, Nanomedicine 5 (2010) 361-368.

[94] M.E. Werner, S. Karve, R. Sukumar, N.D. Cummings, J.A. Coppa, R.C. Chen, et al., Folate-targeted nanoparticle delivery of chemo- and radiotherapeutics for the treatment of ovarian cancer peritoneal metastasis, Biomaterials 32 (2011) 8548-8554.

[95] J. Xie, S. Lee, X. Chen, Nanoparticle-based theranostic agents, Adv. Drug Deliv. Rev. 62 (2010) 1064-1079.

[96] M. Cipreste, A. Peres, A. Cotta, F. Aragon, A. Antunes, A. Leal, et al., Synthesis and characterization of ^{159}Gd-doped hydroxyapatite nanorods for bioapplications as theranostic systems, Mater. Chem. Phys. 181 (2016) 301-311.

[97] H. Zhao, Y. Chao, J. Liu, J. Huang, J. Pan, W. Guo, at al., Polydopamine coated single-walled carbon nanotubes as a versatile platform with radionuclide labeling for multimodal tumor imaging and therapy, Theranostics 6 (2016) 1833-1843.

[98] F. Chen, S. Goel, H.F. Valdovinos, H. Luo, R. Hernandez, T.E. Barnhart, et al., In Vivo integrity and biological fate of chelator-free zirconium-89-labeled mesoporous silica nanoparticles, ACS Nano 9 (2015) 7950-7959.

[99] C.G. England, H-J Im, L. Feng, F. Chen, S.A. Graves, R. Hernandez, et al., Re-assessing the enhanced permeability and retention effect in peripheral arterial disease using radiolabeled long circulating nanoparticles, Biomaterials 100 (2016) 101-109.

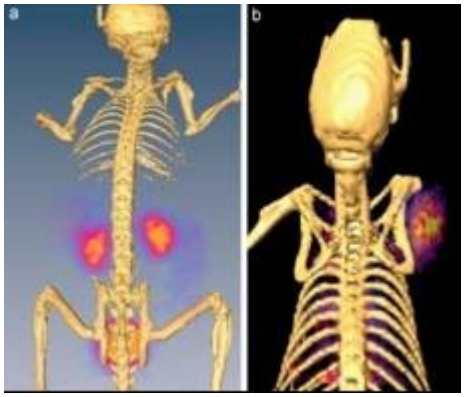

Figure 1

Figure 2

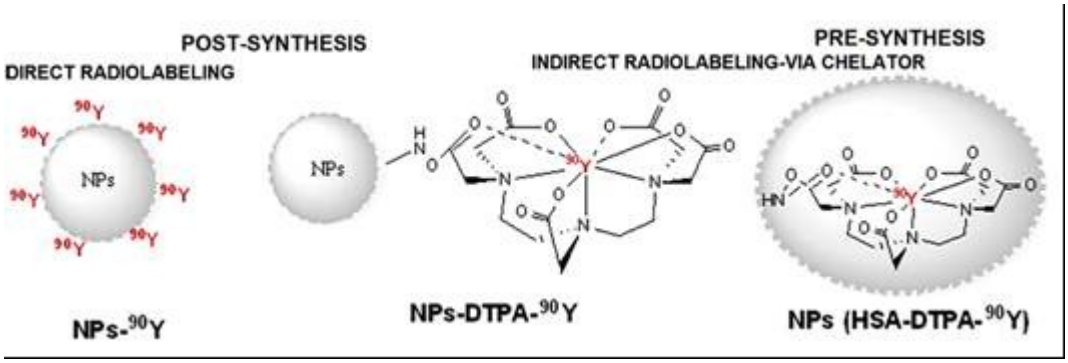

Figure 3

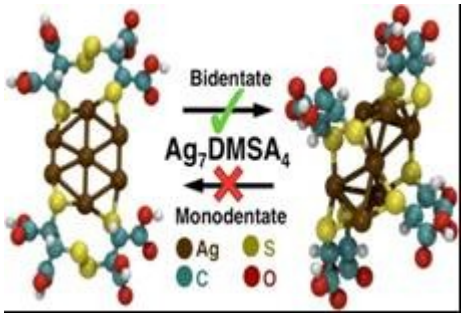

Figure 4

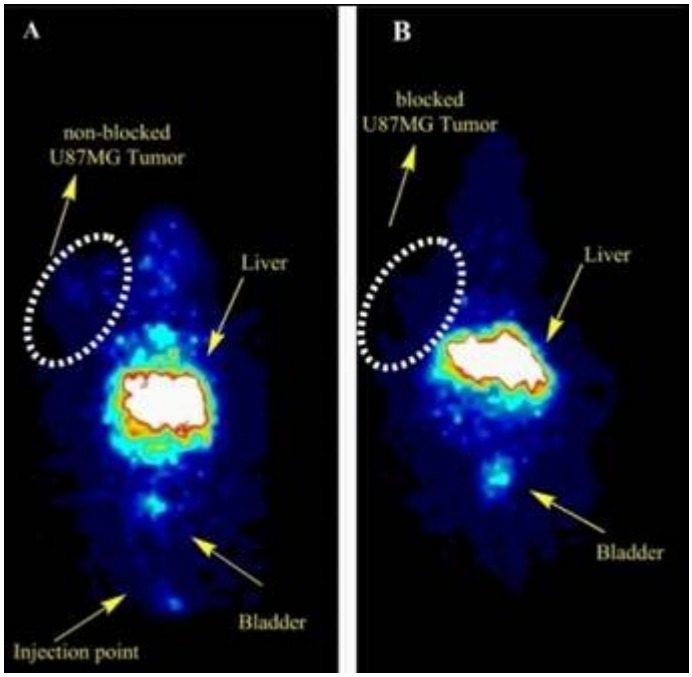

Figure 5

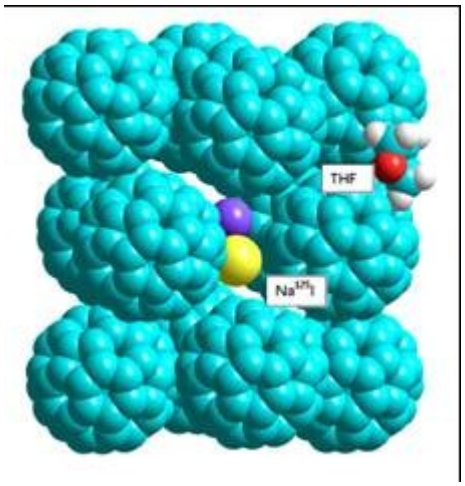

Figure 6

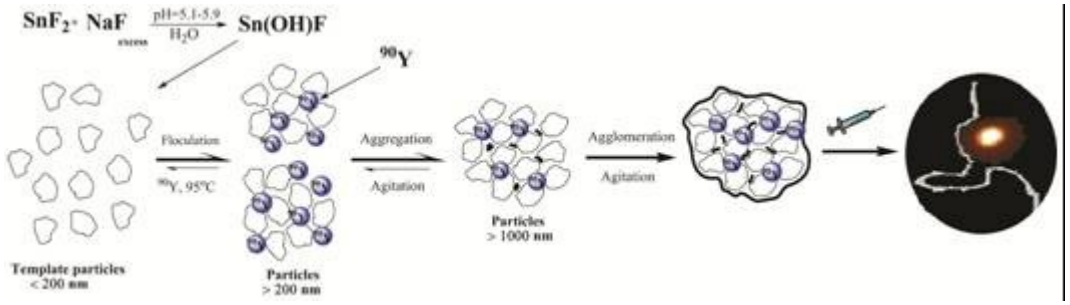

Figure 7

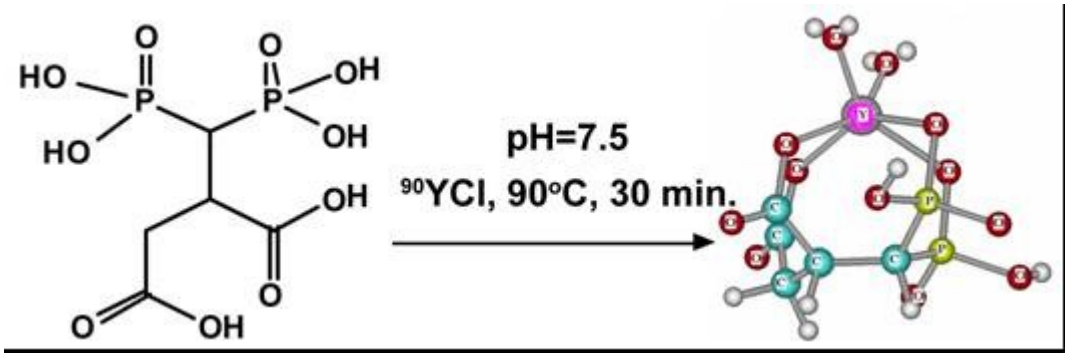

Figure 8

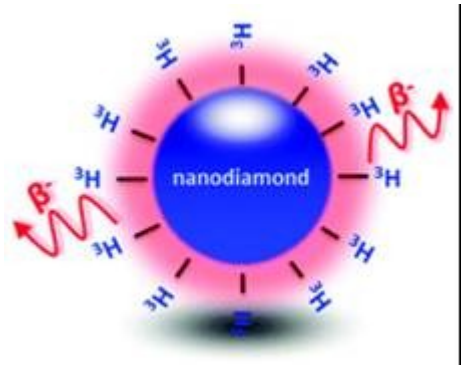

Figure 9

Figure 10

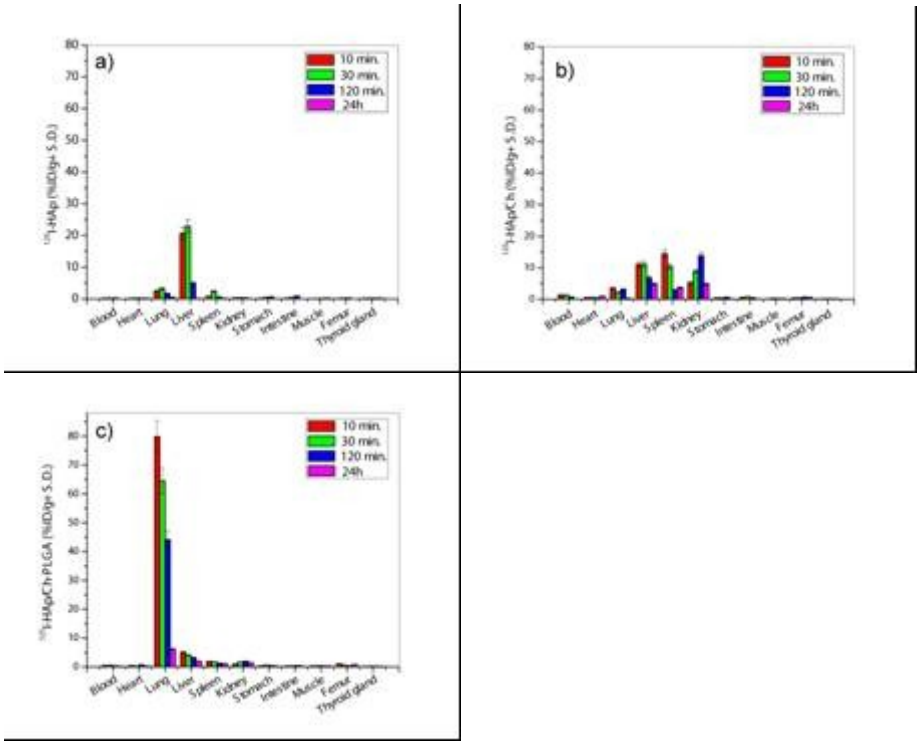

Figure 11

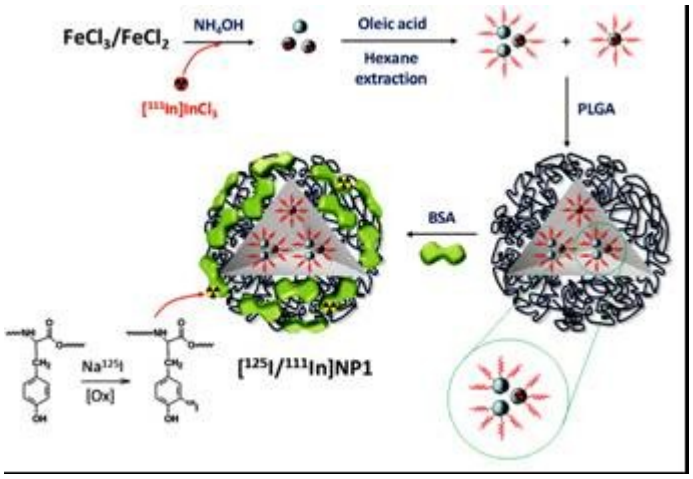

Figure 12

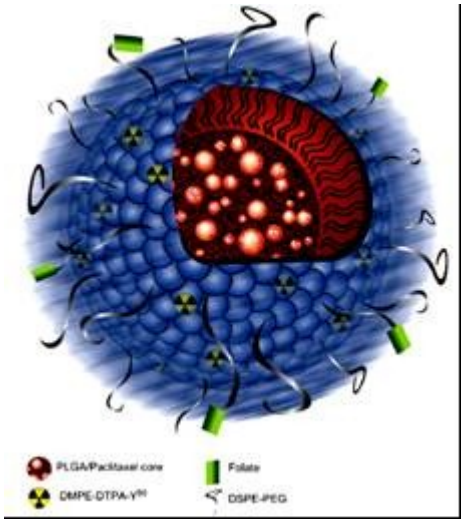

Figure 13

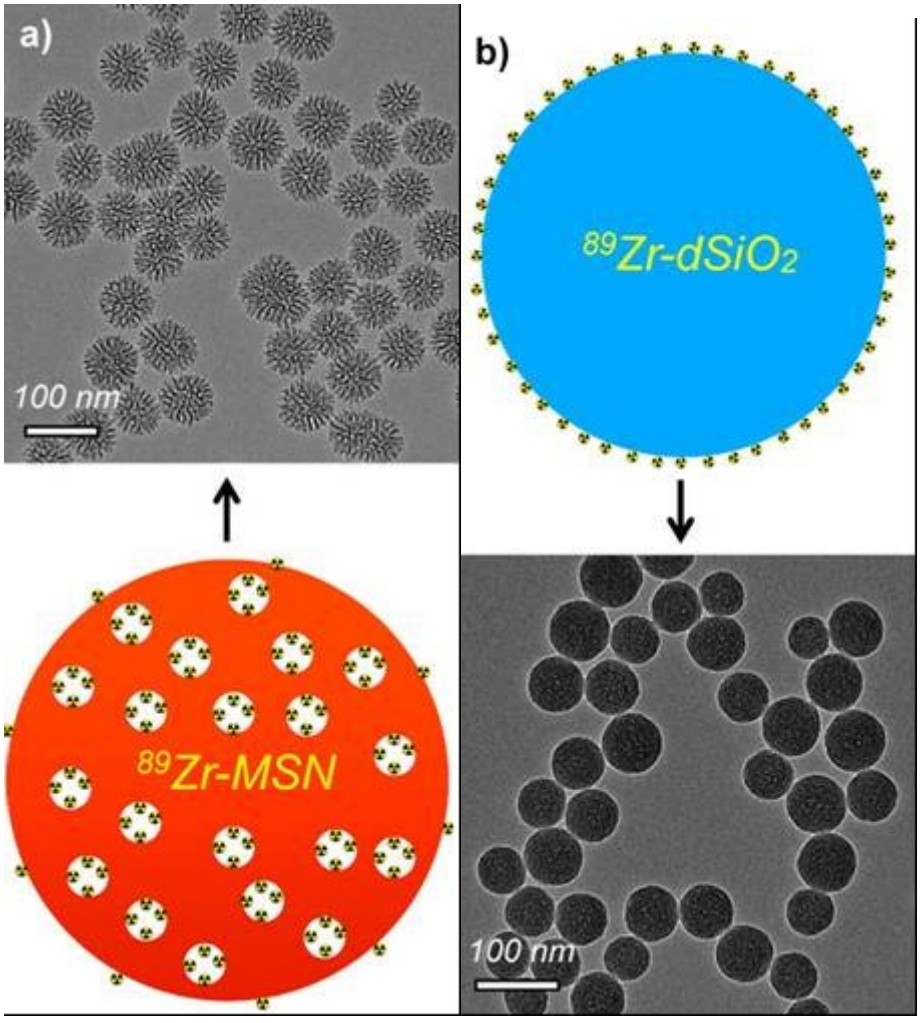

Figure 14